

CNS-accessible Inhibitor of Glucosylceramide Synthase for Substrate Reduction Therapy of Neuronopathic Gaucher Disease

John Marshall¹, Ying Sun^{2,3}, Dinesh S Bangari¹, Eva Budman¹, Hyejung Park¹, Jennifer B Nietupski¹, Amy Allaire¹, Mary A Cromwell¹, Bing Wang¹, Gregory A Grabowski^{2,3}, John P Leonard¹ and Seng H Cheng¹

¹Sanofi Genzyme, Framingham, Massachusetts, USA; ²Division of Human Genetics, Cincinnati Children's Hospital Medical Center, Cincinnati, Ohio, USA; ³Department of Pediatrics, University of Cincinnati School of Medicine, Cincinnati, Ohio, USA.

Gaucher disease (GD) is caused by a deficiency of glucocerebrosidase and the consequent lysosomal accumulation of unmetabolized glycolipid substrates. Enzyme-replacement therapy adequately manages the visceral manifestations of nonneuronopathic type-1 Gaucher patients, but not the brain disease in neuronopathic types 2 and 3 GD. Substrate reduction therapy through inhibition of glucosylceramide synthase (GCS) has also been shown to effectively treat the visceral disease. Here, we evaluated the efficacy of a novel small molecule inhibitor of GCS with central nervous system (CNS) access (Genz-682452) to treat the brain disease. Treatment of the conduritol β epoxide-induced mouse model of neuronopathic GD with Genz-682452 reduced the accumulation of liver and brain glycolipids (>70% and >20% respectively), extent of gliosis, and severity of ataxia. In the genetic 4L;C* mouse model, Genz-682452 reduced the levels of substrate in the brain by >40%, the extent of gliosis, and paresis. Importantly, Genz-682452-treated 4L;C* mice also exhibited an ~30% increase in lifespan. Together, these data indicate that an orally available antagonist of GCS that has CNS access is effective at attenuating several of the neuropathologic and behavioral manifestations associated with mouse models of neuronopathic GD. Therefore, Genz-682452 holds promise as a potential therapeutic approach for patients with type-3 GD.

Received 15 December 2015; accepted 17 February 2016; advance online publication 5 April 2016. doi:10.1038/mt.2016.53

INTRODUCTION

Gaucher disease (GD) is caused by deficient activity of the lysosomal enzyme, glucocerebrosidase (acid β -glucosidase). This results in accumulation of glucosylceramide (GL-1) and its unacylated form glucosylsphingosine (lyso-GL-1), primarily in cells of the monocytic lineage. Disease severity is correlated with the level of residual glucocerebrosidase activity: patients

with higher residual enzyme levels present the nonneuronopathic form referred to as type-1 GD. Patients with lower levels of residual hydrolase activity exhibit neuronal involvement and are termed either as type-2 or -3 GD depending upon the severity of symptoms and life expectancy. Type-2 GD represents the more severe form with earlier disease onset manifesting primarily as central nervous system (CNS) disease with death by 2 years of age. Patients with type-3 GD, also called subacute GD, typically develop visceral involvement first with neurological symptoms developing over time and causing premature death by the second to fourth decade of life.¹

Presently, GD is managed with either enzyme-replacement therapy using recombinant glucocerebrosidase^{2,3} or substrate-reduction therapy (SRT) using miglustat⁴ or eliglustat.⁵ While these therapies address most of the visceral manifestations, none are effective against the CNS disease.⁶ For example, although enzyme-replacement therapy is frequently used as a treatment to alleviate the visceral disease in type-3 GD,^{7–10} no neurological benefit has been demonstrated using this approach. Consequently, a number of different therapeutic strategies are being investigated to address the CNS pathology. These approaches include efforts to reconstitute active glucocerebrosidase in the CNS either by direct delivery of the enzyme into the brain,^{11,12} or through transplantation of bone-marrow¹³ or hematopoietic stem cells.¹⁴ A variety of gene therapy approaches are also being evaluated to treat the neuronopathic disease (reviewed in ¹⁵). Therapies that are based on small-molecule drugs that are able to traverse the blood–brain barrier are also being explored, including chaperone therapy¹⁶ and SRT using miglustat. However, although miglustat is reportedly capable of crossing the blood–brain barrier, it was ineffective when tested in neuronopathic type-3 GD patients.¹⁷ The recently approved eliglustat is not suitable for SRT of the brain disease as it is a substrate of P-glycoprotein (also known as MDR1 or ABCB1) and therefore has poor exposure in the CNS.¹⁸

SRT for GD acts through inhibition of glucosylceramide synthase (GCS) to reduce the production of the substrates GL-1 and lyso-GL-1 that accumulate in the tissues of patients. The therapeutic potential of SRT has been illustrated in mouse models of

type-1^{19,20} and type-2 GD,²¹ but not in putative models of type-3 GD (where there is some residual glucocerebrosidase activity in the CNS). Here, we describe a specific inhibitor of GCS (Genz-682452; GZ/SAR402671) that can access the CNS and that has been demonstrated to effectively lower glycosphingolipid synthesis.²² As such, Genz-682452 represents a potential therapeutic intervention that might benefit the visceral pathologies and also the unmet CNS manifestations observed in type-3 GD that are not addressed by current drugs. The availability of an oral drug that can address the CNS disease would offer several advantages over other approaches being considered such as enzyme-replacement therapy, which is invasive,¹² and transplantation, because of the associated morbidity.²³

Here, we evaluated the efficacy of oral administration of Genz-682452 at inhibiting the accumulation of GL-1 and lyso-GL-1 in the liver and brain in two murine models of neuronopathic GD. One model involved treating mice with the glucocerebrosidase inhibitor, conduritol β epoxide (CBE),²⁴ to generate a surrogate model of neuronopathic GD.^{25–27} This model has previously been used to illustrate the complexity of the bone disease in GD²⁸ and to determine the threshold level of glucocerebrosidase activity needed to prevent the progression of neuronopathic disease.²⁷ It should be noted, though, that off-target effects on other β -glucosidases have been reported for CBE.²⁹ The other murine model of neuronopathic GD used was the transgenic 4L;C* mouse that harbors a homozygous V394L mutation in the *Gba* locus coupled with a knock-in mutation in the saposin C-encoding region.³⁰ This mouse model accumulates GL-1 and lyso-GL-1 in the brain, develops CNS gliosis and exhibits a shortened lifespan (median lifespan of approximately 45 days). We showed that treating these animals with Genz-682452 significantly delayed substrate accumulation and the development of gliosis, as well as neuropathological indicators of disease progression. The findings indicate that SRT using a GCS inhibitor that has brain access may represent an effective approach to treat the CNS manifestations in patients with type-3 GD.

RESULTS

Genz-682452 reduces substrate accumulation in the liver and brain of CBE-induced Gaucher mice

To determine the efficacy of SRT at reducing the substrates (GL-1 and lyso-GL-1) that accumulate in GD, mass spectrometric analysis was performed on liver and hindbrain homogenates obtained from mice treated with CBE, an inhibitor of glucocerebrosidase. As reported previously,³¹ CBE administration to wild-type (WT) C57Bl/6 mice resulted in a decrease in glucocerebrosidase activity and an approximately twofold increase in the amount of GL-1 in the liver (**Figure 1a**). Concomitant administration of the GCS inhibitor, Genz-682452, prevented this elevation in hepatic GL-1. The GL-1 levels observed at the end of the 7-week treatment period were approximately 20% of those in untreated control mice (**Figure 1a**). Hepatic lyso-GL-1 levels were also highly elevated (~100-fold increase) in CBE-treated mice compared with untreated control mice (**Figure 1b**). Genz-682452-mediated SRT of CBE-treated mice significantly reduced the elevated levels of hepatic lyso-GL-1 by approximately 75% (**Figure 1b**).

Mass spectrometric measurements of GL-1 in the hindbrains of CBE-treated C57Bl/6 mice showed an approximately 10-fold

higher level of the glycolipid compared with the untreated controls (**Figure 2a**). SRT of CBE-treated animals resulted in an approximately 25% reduction in total GL-1 levels, although this did not reach statistical significance (**Figure 2a**). Further analysis of the different GL-1 isoforms in the brain revealed that the majority (~80%) of the isoforms that were increased by CBE treatment were those with shorter ceramide acyl chain lengths (<21 carbons long; **Figure 2b**). Whereas Genz-682452 treatment did not significantly lower the levels of these isoforms, the levels of GL-1 species that were longer than 21 carbons were significantly reduced (by ~50%) (**Figure 2c**). These longer isoforms (>21 carbons long) represent glycosphingolipids from cell types that predominantly express ceramide synthase 2, which are associated with the white matter in the CNS. Similar to what was seen in the liver, there was a >100-fold increase in the brain level of lyso-GL-1 in the brains of CBE-treated mice. Treatment with Genz-682452 significantly lowered these levels by approximately one-third (**Figure 2d**). Hence, Genz-682452-mediated SRT was effective at reducing the accumulation of substrates in the liver and brain of CBE-induced Gaucher mice.

Genz-682452 reduces the extent of gliosis in the brains of CBE-induced Gaucher mice

Brains were harvested from the mice at the end of the 7-week study and sections then immunostained with either anti-CD68 or anti-GFAP antibodies to identify microglia and astrocytes, respectively. **Figure 3a** shows representative sections from the striatum though other areas of the brain were evaluated (including the cortex, hippocampus, substantia nigra, and cerebellum) with similar findings. Increased intensity and area of staining for both microglia and astrocytes were observed in the CBE-treated mice compared to the control animals. A significantly lower extent of gliosis was apparent in the CBE- and Genz-682452-treated group than in the CBE only-treated cohort, either visually (**Figure 3a**) or following quantification using image analysis software (**Figure 3b**). The extent of microglial infiltration, as illustrated by staining for CD68⁺ cells, was also significantly reduced in the CBE-treated mice that were administered Genz-682452 (**Figure 3a,b**). Hence, Genz-682452-mediated lowering of glycosphingolipids in the CNS correlated with a concomitant decrease in the extent of gliosis.

Genz-682452 partially corrects a behavioral aberration (hind limb splay) in the CBE-induced mouse model of GD

One of the phenotypic characteristics of CBE-induced Gaucher mice is a deficit in the natural splay response of their hind limbs upon suspension by the tail.³¹ This aberration is also a feature of other mouse models of neurodegenerative disease.^{32–34} Animals were evaluated periodically in a blinded manner using a severity scoring system that reflected the degree to which they were able to splay their hind limbs (**Figure 4**). Healthy WT mice typically exhibited a broad splay of their limbs upon being suspended by their tail. In contrast, CBE-treated mice showed a progressive deterioration with age as illustrated by an increased tendency to draw their hind limbs to midline and to clench their hind paws. Treating the CBE-induced Gaucher mouse with Genz-682452

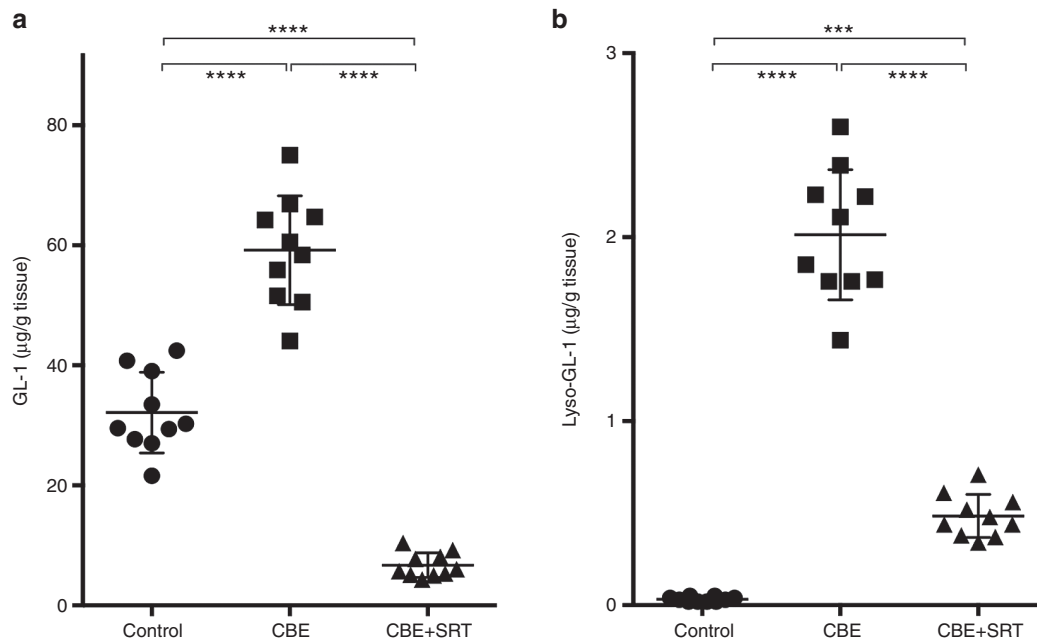


Figure 1 Effect of SRT on liver GL-1 and lyso-GL-1 concentrations in CBE-treated C57Bl/6 mice. Livers from untreated (control), CBE-treated (dosed IP at 100 mg/kg/day) (CBE), and CBE- and Genz-682452-treated (dosed in the diet at ~60 mg/kg/day) (CBE+SRT) C57Bl/6 mice were analyzed to determine levels of GL-1 (**a**) and lyso-GL-1 (**b**) at the end of the study period (after 7 weeks of treatment, which corresponded to 11 weeks of age). Individual data points ($n = 10$ per group) and mean \pm SD are presented. Data were analyzed using one-way ANOVA with Tukey's post-test; *** $P < 0.001$, **** $P < 0.0001$. CBE, conduritol β epoxide; GL-1, glucosylceramide; SRT, substrate reduction therapy.

resulted in a significant delay in progression of this aberrant behavior, albeit not to the level noted in control animals. This suggests that Genz-682452-mediated lowering of lysosomal storage of glycosphingolipids and gliosis in the brain of Gaucher mice could translate to an improvement in their neurobehavioral disorder.

Genz-682452 reduces accumulation of substrate in the liver and brain of 4L; C^* Gaucher mice

The positive impact of SRT in the CBE-induced model of neuronopathic GD was confirmed in the 4L; C^* mouse, a genetic murine model of type 2/3 GD that typically only survives for approximately 45 days.³⁰ In this study, 4L; C^* mice were subjected to daily intraperitoneal injections of Genz-682452 starting at 5 days of age until day 20, after which they were then provided the drug in their food pellets. Quantitative analysis of GL-1 and lyso-GL-1 levels in the liver and brain of 4L; C^* mice and their control littermates (4L/WT) were determined when the animals were 21, 35, 45, and 65 days of age. Levels of GL-1 in the hindbrain of untreated 4L; C^* mice (on days 21, 35, and 45) were determined to be approximately fivefold higher than in the 4L/WT controls (Figure 5a). Administration of Genz-682452 to the 4L; C^* mice starting at 5 days of age resulted in approximately 50% lower levels of GL-1 than their untreated counterparts on days 21, 35, and 45 (Figure 5a). The brain levels of lyso-GL-1 in the 4L; C^* were also highly elevated relative to control mice and these levels increased progressively as the animals aged (Figure 5b). Treatment with Genz-682452 also lowered the lyso-GL-1 levels to approximately 50% of those in the untreated counterparts at all time points measured (Figure 5b). It should be noted that Genz-682452 was only able to delay and not halt the accumulation of lyso-GL-1 as the overall levels of the lipid in the brain continued to increase with age (Figure 5b).

Measurement of GL-1 levels in the liver of 4L; C^* mice showed they were elevated two to threefold over those of control animals (Figure 5c). As observed earlier with the CBE-induced mouse model of GD, treatment of the 4L; C^* mice with Genz-682452 lowered GL-1 to below 4L/WT levels (Figure 5c). There were no overt toxicities associated with the chronic suppression of liver GL-1 levels to below normal based on the observations of their daily activity and body weight data. Levels of liver lyso-GL-1 in untreated 4L; C^* mice were also highly elevated relative to control mice, and treatment with Genz-682452 reduced this by >70% at all time points measured (Figure 5d). Hence, the efficacy of SRT noted in the CBE-induced mouse model was also realized in the genetic murine model of neuronopathic GD.

Genz-682452 reduces the extent of CD68⁺ staining in the brain of 4L; C^* Gaucher mice

Brain sections were prepared from untreated and Genz-682452-treated 4L; C^* mice as well as from control mice (at 21, 35, 45, and 65 days of age) and then immunostained using an anti-CD68 antibody. Figure 6a shows representative images of stained sections from the spinal cord and brain stem of 45-day-old mice. Untreated 4L; C^* mice showed a greater extent of CD68⁺ staining in both the brain stem and spinal cord than control mice, indicating an increased number of microglia in the CNS of Gaucher mice. The intensity and number of CD68⁺-stained microglia were significantly reduced in Genz-682452-treated 4L; C^* mice (Figure 6a). Quantitative analysis of sections at different time points indicated that the increase in microglia in the spinal cord, brain stem, and thalamus of untreated 4L; C^* mice was rapidly progressive with age (Figure 6b); similar data were noted in the cerebellum, cortex, and striatum (data not shown).

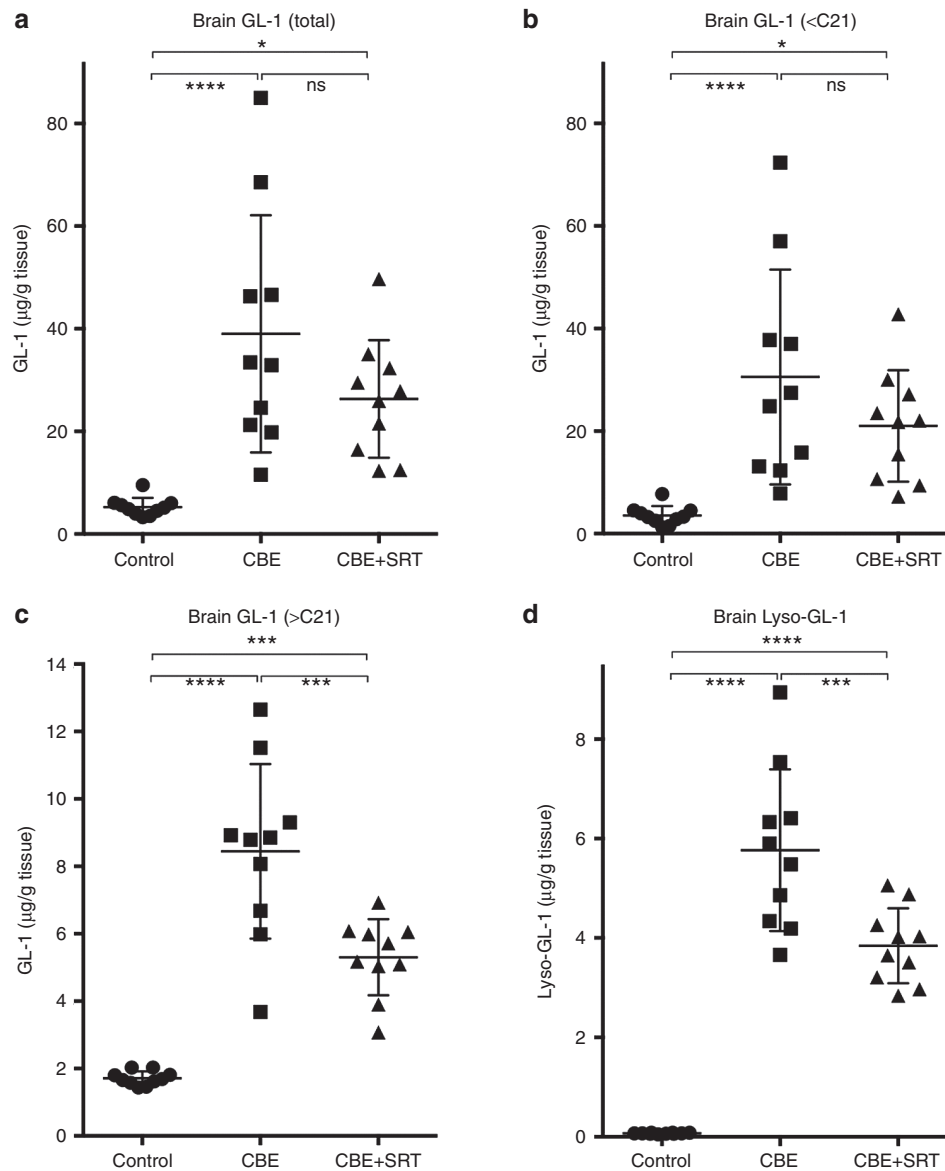


Figure 2 Effect of SRT on GL-1 and lyso-GL-1 concentrations in the hindbrains of CBE-treated C57Bl/6 mice. The hindbrain from untreated (control), CBE-treated (dosed IP at 100 mg/kg/day) (CBE), and CBE- and Genz-682452-treated (dosed in the diet at ~60 mg/kg/day) (CBE+SRT) C57Bl/6 mice were analyzed for total GL-1 (**a**), GL-1 isoforms with an acyl chain carbon length of <21 (**b**), GL-1 isoforms with an acyl chain carbon length of >21 (**c**), and lyso-GL-1 (**d**) at the end of the study period (after 7 weeks of treatment, which corresponded to 11 weeks of age). Individual data points ($n = 10$ per group) and mean \pm SD are presented. Data were analyzed using one-way ANOVA with Tukey's post-test; ns = not significant, * $P < 0.05$, *** $P < 0.001$, **** $P < 0.0001$. CBE, conduritol β epoxide; GL-1, glucosylceramide; SRT, substrate reduction therapy.

In contrast, 4L;C* mice treated by SRT showed lower levels of CD68⁺ cells at 45 and 65 days of age. The extent of CD68-staining in control mice was low and remained unchanged throughout the course of this study.

Genz-682452 treatment delays the onset of gait abnormalities and increases longevity of 4L;C* Gaucher mice

4L;C* mice develop a gait abnormality that is illustrated by an aberrant limb stride length and spacing of their hind limbs (base). This leads to a significant reduction in the length of both their left and right strides, particularly as they approach end-stage disease

(**Figure 7a**). Onset of aberrant gait, which is indicative of neurodegenerative disease, was clearly evident in untreated 4L;C* mice starting at 30 days of age and it became progressively worse with age. Interestingly, treatment of 4L;C* mice with Genz-682452 delayed the onset of these abnormalities until the mice were over 50 days old (**Figure 7a,b**). Importantly, in contrast to untreated 4L;C* mice which had a median survival of approximately 45 days,³⁰ treatment with Genz-682452 increased this to over 60 days, which represents an approximately 30% increase in longevity (**Figure 7c**). Hence, SRT of 4L;C* mice resulted in lower levels of lysosomal glycosphingolipid storage and of CD68⁺ microglial staining in the CNS and that translated to an increase in longevity.

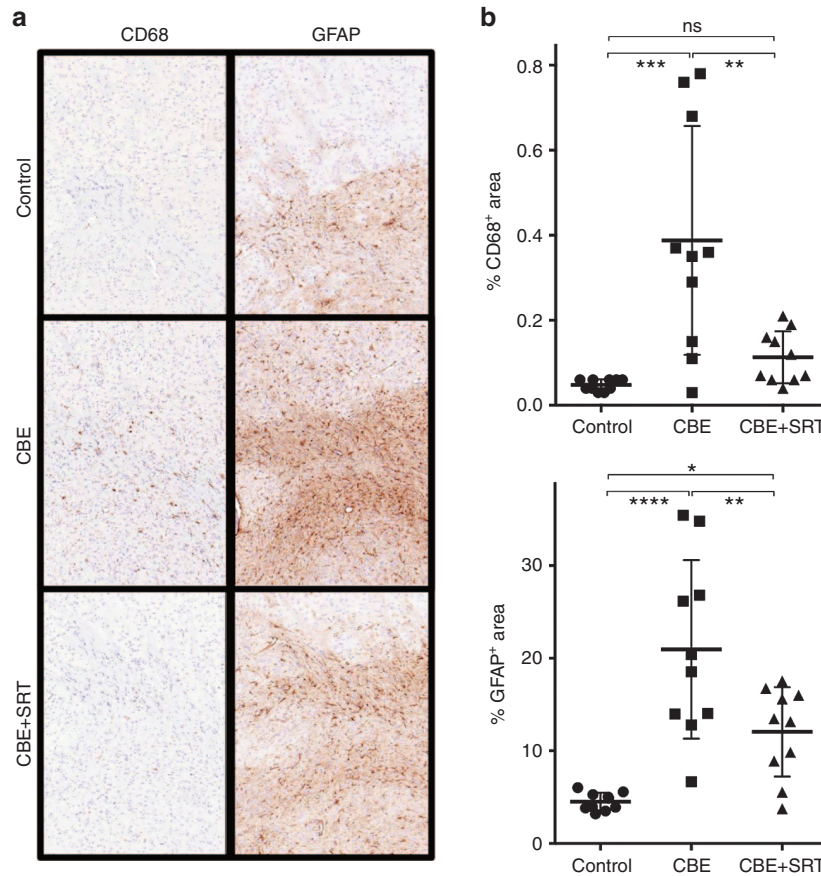


Figure 3 Effect of SRT on the extent of gliosis in the striatum of CBE-treated C57Bl/6 mice. Brains were harvested from untreated (control), CBE-treated (dosed IP at 100mg/kg/day) (CBE), and CBE- and Genz-682452-treated (dosed in the diet at ~60mg/kg/day) (CBE+SRT) C57Bl/6 mice at the end of the study period (after 7 weeks of treatment, which corresponded to 11 weeks of age) and subjected to immunohistochemical staining to identify microglia (CD68 staining) and astrocytes (GFAP staining). Sections of striatum are shown; brown coloration indicates positive staining for CD68 or GFAP (a). Quantification of percent area staining positively for CD68 and GFAP from 10 representative sections is shown (b). Data were analyzed using one-way ANOVA with Tukey’s post-test; ns = not significant, **P* < 0.05, ***P* < 0.01, ****P* < 0.001, *****P* < 0.0001. CBE, conduritol β epoxide; SRT, substrate reduction therapy.

DISCUSSION

While the visceral manifestations associated with type-1 GD can be effectively managed by current enzyme and substrate reduction therapies, they do not adequately address the CNS disease in type-2 and -3 GD patients.^{6,35} Chaperone therapy has shown early promise as a treatment for neuronopathic GD,³⁶ particularly those harboring the most common type-3-associated *GBA* mutation L444P³⁷; however, subsequent clinical studies were halted due to lack of efficacy. Systemic administration of very high doses of recombinant glucocerebrosidase has also been attempted in type-3 GD patients, but this did not impact CNS symptoms because the enzyme could not efficiently traverse the blood–brain barrier.^{9,10} Preclinical studies of direct intracerebroventricular or intraparenchymal delivery of enzyme in neuronopathic models of Gaucher mice have shown improved functional outcomes³⁸ but chronic CNS delivery would be clinically challenging. SRT, for which there are two approved drugs, is a clinically validated approach for treating GD; miglustat⁴ was approved for type-1 GD as a second-line therapy, and more recently eliglustat⁵ received approval for type-1 GD as a first-line therapy. SRT using the CNS-accessible small-molecule drug, miglustat, was evaluated in a controlled trial of type-3 Gaucher patients but no effect on brain

disease was observed, presumably because the exposure levels in the CNS were inadequate.¹⁷ As such, a more potent, selective, and CNS-accessible small molecule may confer a better outcome. Here, we described our findings with a novel and potent inhibitor of GCS (Genz-682452) that has CNS access in two mouse models of neuronopathic GD.

Although several mouse models of GD have been developed,^{39,40} most of the neuronopathic models exhibit an acute disease onset and early death that is more reminiscent of patients with type-2 GD. Few exhibit a neuronopathic phenotype that reflects the disease observed in patients with type-3 disease. For this reason, we elected to evaluate the merits of SRT in a CBE-induced mouse model in which the severity of symptoms can be moderated based on the age of the mouse at the start of CBE treatment, the mouse strain, and also the dose and frequency of dosing of the CBE. Due to reported off-target effects of CBE²⁹, we also confirmed the observations using a genotypic model of neuronopathic GD, which exhibits a chronic phenotype. The CBE model has been reported to exhibit features of both the visceral and neuronopathic sequelae in GD.^{25,41,42} Here, we showed that administering CBE to C57Bl/6 mice resulted in the progressive development of a CNS phenotype, as illustrated by gliosis and an aberrant hind

limb splay, both of which worsened with age. The Gaucher 4L;C* mouse, which has reduced glucocerebrosidase activity (resulting from the V394L mutation and a knock-in mutation in the saposin C region of the prosaposin locus), is also reported to exhibit several disease features that have been observed in patients with type-3 GD.^{30,36,43}

In both the chemically induced and genotypic mouse models of GD, liver GL-1 levels were determined to be elevated by approximately two to threefold that of WT mice. In the brain, GL-1 levels were also significantly higher in the CBE-induced mice (~10-fold higher than WT mice) than in the 4L;C* mice (approximately fivefold higher than WT mice). This difference in the extent of elevation in the liver and brain may be due to the differential levels of synthesis of glucocerebrosidase in the respective organs. For example, it has been reported that a single intraperitoneal administration of 100 mg/kg of CBE effectively inhibited glucocerebrosidase activity to <5% of untreated control levels. Activity measurements performed after 24 hours of CBE treatment showed that glucocerebrosidase levels were restored to ~20% of normal in the liver but to only ~10% of normal levels in the CNS.^{27,44} In the 4L;C* mouse, the residual glucocerebrosidase activity was ~10% of that in WT mice in both the liver and brain,³⁰ and this reduction may therefore be expected to result in the accumulation of similar levels of GL-1 in both tissues. Irrespective of

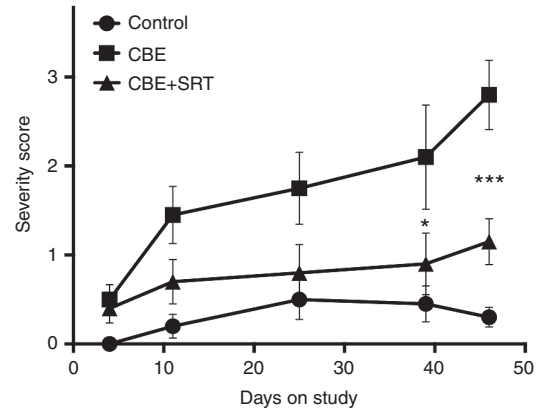


Figure 4 Effect of SRT on hind limb splay in CBE-treated C57Bl/6 mice. The hind limb splay response was observed by suspending mice by their tails and was assessed in a blinded manner using a scale of 0 (normal WT response) to 5 (severe deficit with no splay response). The splay response of untreated (control), CBE-treated (dosed intraperitoneally at 100 mg/kg/day) (CBE), and CBE- and Genz-682452-treated (dosed in the diet at ~60 mg/kg/day) (CBE+SRT) C57Bl/6 mice was assessed at the indicated time points. Higher numbers indicate a greater deviation from the normal response (lesser extent of hind limb splay and increased paw clenching). Data were analyzed using one-way ANOVA with Tukey's post-test between the CBE and CBE+SRT groups; **P* < 0.05, ****P* < 0.001. CBE, conduritol β epoxide; SRT, substrate reduction therapy; WT, wild-type.

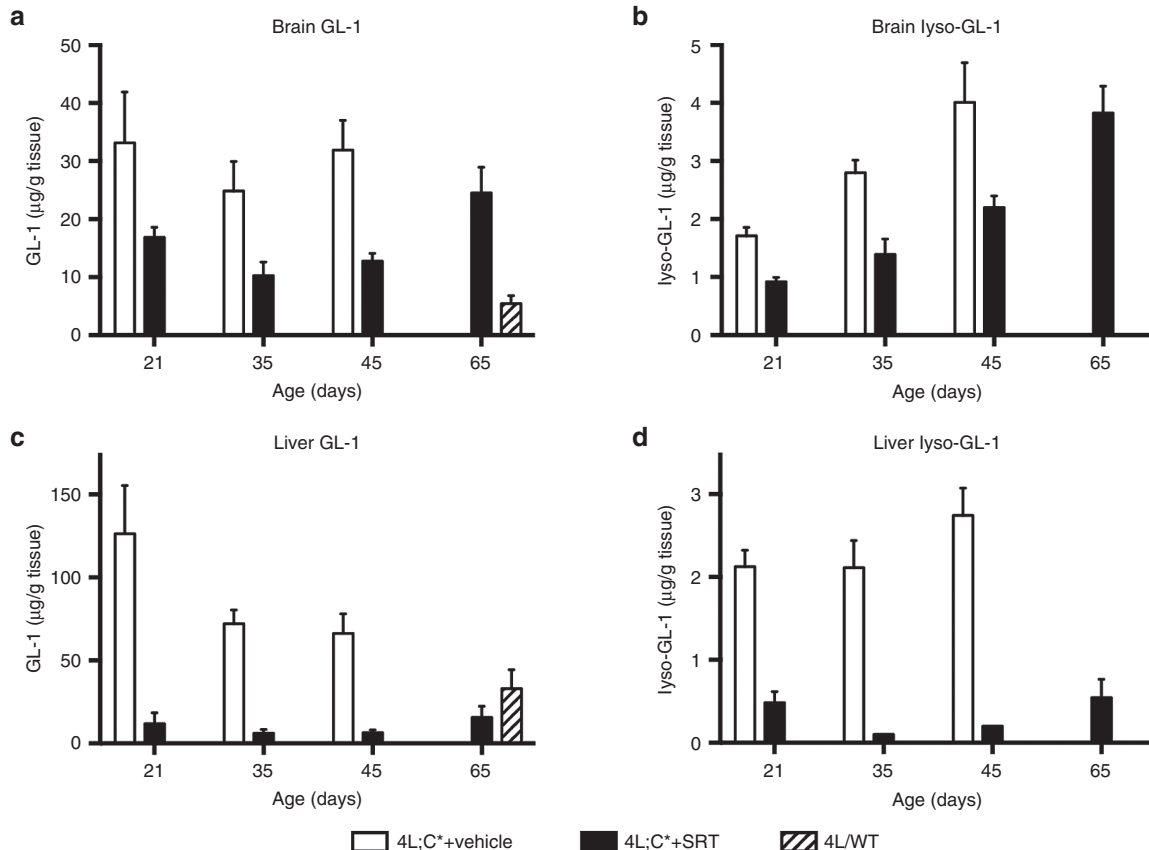


Figure 5 Effect of SRT on GL-1 and lyso-GL-1 concentrations in the hindbrain and liver of 4L;C* mice. Hindbrain and liver from untreated 4L/wild-type mice (4L/WT), vehicle-treated 4L;C* (4L;C*+vehicle), and Genz-682452-treated 4L;C* mice (4L;C*+SRT) were analyzed to determine levels of GL-1 in the hindbrain (a), lyso-GL-1 in the hindbrain (b), GL-1 in the liver (c), and lyso-GL-1 in the liver (d). Genz-682452 was dosed IP at 12.5 mg/kg/day from days 5 to 20 and at ~60 mg/kg/day in diet thereafter; *n* ≥ 6 mice per group. GL-1, glucosylceramide; SRT, substrate reduction therapy.

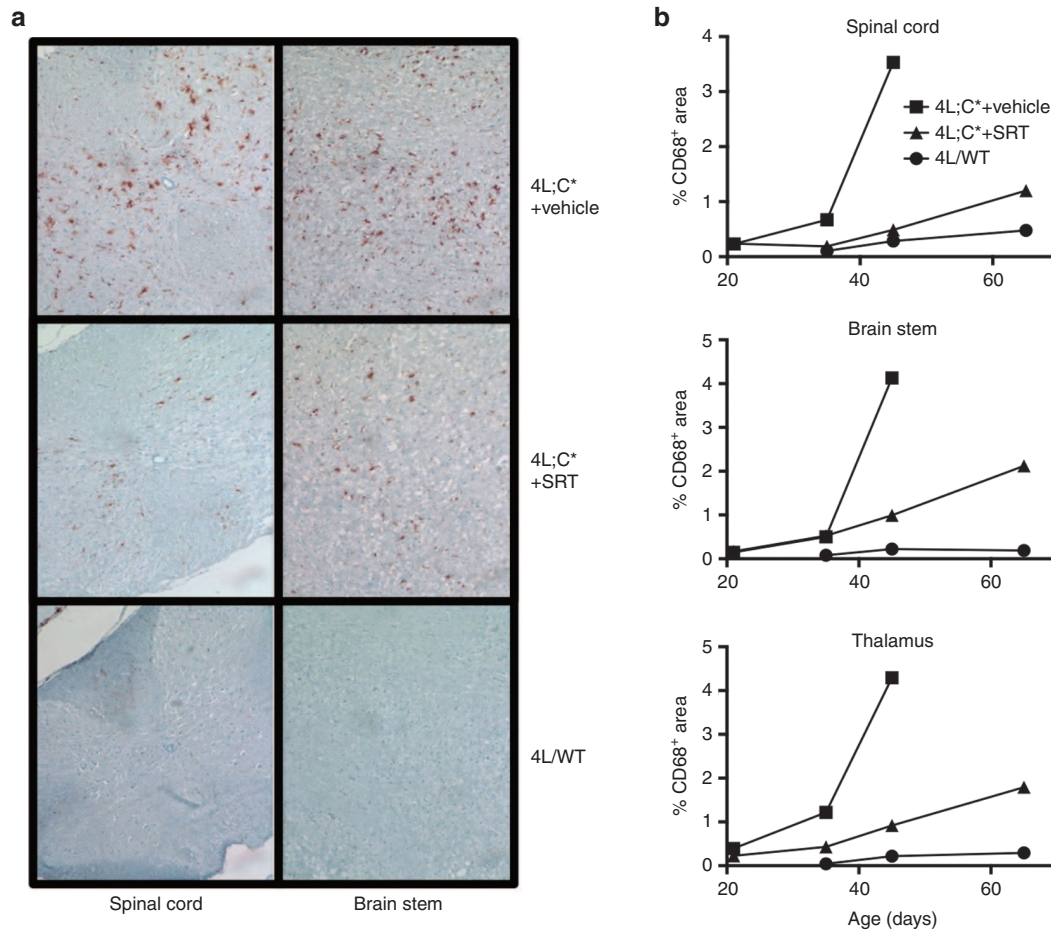


Figure 6 Effect of SRT on the extent of CD68 staining in the CNS of 4L;C* mice. CNS from 45-day-old untreated 4L/wild-type (4L/WT), vehicle-treated 4L;C* (4L;C*+ vehicle), and Genz-682452-treated 4L;C* (4L;C*+SRT) mice were subjected to immunohistochemical analysis to identify microglia (CD68 staining). Genz-682452 was dosed IP at 12.5 mg/kg/day from days 5 to 20 and at approximately 60 mg/kg/day in diet thereafter. Sections of spinal cord and brainstem are shown; brown coloration indicates positive staining for CD68 (a). Quantifications of percent area staining positively for CD68 in representative sections of the spinal cord, brainstem, and thalamus are shown for tissues taken at 21-, 35-, 45- and 65-days old (b). CNS, central nervous system; SRT, substrate reduction therapy.

the mouse model used, SRT reduced liver GL-1 levels to below those in WT mice and, importantly, reduced the level of GL-1 in the brain by 30–50%. This result demonstrated that Genz-682452 was efficacious at lowering GL-1 levels in both tissue compartments. As such, Genz-682452 represents a potentially new and practical (as it is orally available) therapeutic intervention that might address both the visceral pathologies and the unmet CNS manifestations observed in type-3 GD.

The observation of different glycolipid isoforms in the CNS and liver is likely the result of differential cellular expression patterns of the various ceramide synthases. Ceramide synthase 1, which is primarily responsible for generating the C18 ceramide isoform is the most abundant of the ceramide synthases in mouse brain.⁴⁵ This is consistent with our observations that in the mouse brain, ~70% of the GL-1 is comprised of the C18 isoform. CerS2, which generates mainly the C22 and C24 ceramide isoforms is highly expressed in white matter tracts including those of the cerebellum and brain stem.⁴⁵ Analysis of brain tissue from a patient with type-3 GD revealed that the isoforms of accumulated GL-1 were predominantly those with longer acyl chains (>20 carbons).¹⁰ These longer chain isoforms were primarily impacted by SRT in

the CBE-induced Gaucher mouse, suggesting that perhaps Genz-682452 was preferentially active in cell types that are relevant to type-3 GD. Interestingly, a reduction of the longer chain GL-1 isoforms in the hindbrain (which includes the cerebellum and brain stem) of SRT-treated mice correlated with a delay in hind-limb deficits, suggesting that the behavioral aberration may be related to the observed cerebellar pathology.

The neurotoxic activity of lyso-GL-1 has been postulated to be causative of the disease in neuronopathic GD^{46–49} but how it manifests at a physiological level remains unclear. It should be noted that neuronal GL-1 levels have been implicated as the cause of neuropathological changes *in vivo*,⁵⁰ although this was in a mouse model lacking glucocerebrosidase in only the neurons and macroglia. Here, we showed that lyso-GL-1 levels in the brain and liver are highly elevated in both mouse models of neuronopathic GD and that they were significantly reduced by SRT. Interestingly, in the 4L;C* mouse, in support of a role of lyso-GL-1 in the CNS disease, the survival of the mice correlated more closely with the absolute levels of lyso-GL-1 than with GL-1. Moreover, the neurobehavioral deficits (hind-limb splay and gait) in both CBE-induced and 4L;C* mouse models were responsive

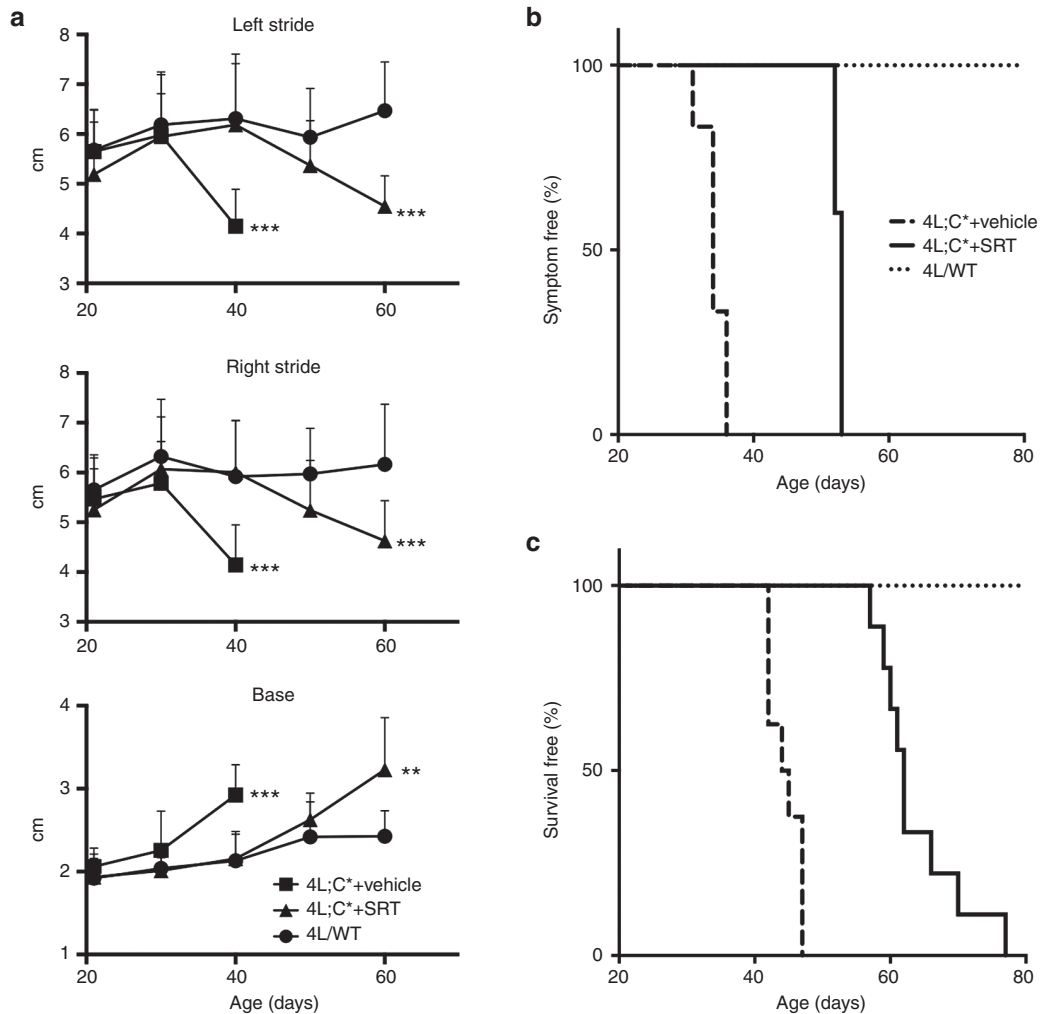


Figure 7 Effect of SRT on gait and longevity of 4L;C* mice. The stride length and distance between the rear paws (base) were periodically measured starting when the mice were 21 days old (**a**). Data were analyzed using Student's *t*-test to compare the 4L;C*+vehicle and 4L/WT or 4L;C*+SRT (Genz-682452 dosed IP at 12.5 mg/kg/day from days 5 to 20 and at approximately 60 mg/kg/day in diet thereafter) and 4L/WT; ** $P < 0.01$, *** $P < 0.001$. The age of disease onset was determined by a significant deviation in gait from that of the 4L/WT mice and is shown as the percent of mice that remained symptom-free (normal gait) at the indicated age (**b**). The difference between 4L;C*+vehicle and 4L;C*+SRT is highly significant ($P < 0.0001$) by log-rank (Mantel-Cox) test. The percent of mice that had not reached the criteria for sacrifice at the indicated age is shown in the survival curve (**c**). The difference between 4L;C*+vehicle and 4L;C*+SRT is highly significant ($P < 0.0001$) by log-rank (Mantel-Cox) test. SRT, substrate reduction therapy.

to treatment with Genz-682452. The degree of deficit in the gait of the 4L;C* mice was similar in Genz-682452-treated and untreated mice at their respective end-stage of disease. This phenotypic characteristic also correlated more closely with the levels of lyso-GL-1 than GL-1 in the CNS or with the degree of gliosis, further supporting the role of lyso-GL-1 as the pathogenic agent. If true, future efforts should seek to validate lyso-GL-1 as a potential surrogate biomarker of neuronopathic GD.

The observation of gliosis (as measured by increases in CD68 (microglial) and GFAP (astrocyte) staining) in these mouse models of GD has been reported previously.^{30,51} Gliosis is thought to occur as a consequence of the inflammatory signals that are elicited by neuronal accumulation of GL-1 and lyso-GL-1.⁵⁰ Our studies showed that SRT could significantly delay the onset and progression of gliosis throughout the CNS. Intriguingly, in the Genz-682452-treated 4L;C* mouse at end stage (day 65), the level of CD68 staining was much less than that seen in untreated mice

at the same stage (day 45) (Figure 6). This suggested that the levels of lyso-GL-1, which were similar at end stage of treated and untreated 4L;C* mice, may not be solely responsible for the gliosis observed in the CNS.

In summary, the data here strongly support the use of SRT based on specific inhibition of GCS as an approach to managing subacute neuronopathic GD (type-3). The clinical validation of SRT as a therapeutic approach, as evidenced by the successful treatment of visceral manifestations in type-1 GD patients receiving eliglustat, supports the use of a similar approach with a CNS-accessible small molecule for type-3 GD. However, measuring clinical efficacy in type-3 GD patients presents many challenges. These include the high degree of variability in symptoms that has been observed between patients, the variable rate of disease progression, the irreversible nature of the neurodegenerative changes, and the paucity of CNS-related biomarkers that could serve as a surrogate endpoint. Unlike type-1 GD, which has

objective clinical outcome measures that are indicative of therapeutic efficacy, no such measures have yet been validated for the neuronopathic forms of the disease. Measurement of saccadic eye movement velocity, which was used to determine the efficacy of miglustat for Niemann–Pick C disease,⁵² may represent one potential assay for type-3 GD.⁵³ In addition, recent improvements in analytical methodologies have led to the identification of glycolipid fluctuations in the cerebrospinal fluid of GD patients^{11,54} as well as other potential biomarkers⁵⁵ that may be used to track the progression of clinical disease. Finally, because GCS catalyzes the first step in glycosphingolipid synthesis this therapeutic strategy, if successful, may be extended to include other related glycosphingolipidoses, such as late-onset Tay–Sachs and Sandhoff diseases.

MATERIALS AND METHODS

Animal procedures. Procedures involving mice were reviewed and approved by the Institutional Animal Care and Use Committee of Sanofi Genzyme following guidelines established by the Association for Assessment of Accreditation of Laboratory Animal Care (AAALAC). WT C57Bl/6 mice were obtained from Taconic Laboratories (Germantown, NY).

The chemically induced GD model was generated by administering CBE, an inhibitor of glucocerebrosidase, to C57Bl/6 mice (female, 10 mice/group). Dosing was via daily intraperitoneal injections of 100 mg/kg CBE starting at 4 weeks of age for 7 weeks. Concurrent with the administration of CBE, mice received Genz-682452 as a component of their standard pelleted rodent diet (Genz-682452 was formulated at 0.03% w/w in LabDiet 5053 (TestDiet, Richmond, IN)). This formulation provided approximately 60 mg of Genz-682452/kg/day for a 20-g mouse eating 4 g of food per day. This dose was selected based on earlier pilot studies (data not shown) in a mouse model of Fabry disease.²² The second GD model, the 4L;C* mouse, harbors a *Gba* V394L mutation and lacks saposin C as described previously.³⁰ This mouse model exhibits onset of disease symptoms at approximately 30 days of age and has a median survival of approximately 45 days. Drug delivery was initially facilitated via daily intraperitoneal injections of 12.5 mg/kg of Genz-682452 between days 5 and 20 and thereafter as a component of the pelleted diet (0.03% w/w), as described above for the CBE model.

Hind limb splay, a recognized test of CNS dysfunction, was performed on the chemically induced Gaucher mice in a blinded manner using a severity score scale of 0–5 to indicate the degree of deviation from normal animals. Mice were suspended by the tail and the splay posture was scored as follows: a score of 0 was assigned to WT mice, which typically show a completely splayed posture with toes extended. A score of 5 was assigned to mice whose hind limbs were consistently drawn in and whose paws were clenched. This phenotype has previously been described in CBE-induced Gaucher mice.³¹

Progression of aberrant neurobehavioral phenotype in the 4L;C* mice was determined by assessing their sensorimotor function using gait analysis as previously described.⁵⁶ Mice were trained to walk through a narrow alley leading into their home cage. Once trained, a piece of paper was placed on the alley floor. The hind paws of the mouse were brushed with nontoxic paint and then allowed to walk through the alley. Their stride length was determined by measuring the distance between hind paw prints recorded on the paper. The base measured the distance between the left and right paw. Only strides made while continuously walking (no stopping) for at least three strides in each test were recorded for the analysis. Treated 4L;C* mice were compared to age-matched untreated 4L;C* by Student's *t*-test using GraphPad Prism 5. Mice were killed when they reached a humane endpoint (inability to self-nourish and >20% loss of body weight).

Sphingolipid analysis. Quantitative analysis of sphingolipids was performed by liquid chromatography and tandem mass spectrometry (LC/MS/MS).

Briefly, tissue was homogenized in 10 volumes of water (w/v) after which a 10- μ l aliquot of the homogenate was extracted with 1 ml of an organic solvent mixture. For GL-1 analysis, 10 μ l of homogenate was extracted with 1 ml of 90% mobile phase A (96:2:1:1 acetonitrile/methanol/acetic acid/water (v/v/v/v)) and 10% mobile phase B (98:1:1 methanol/acetic acid/water (v/v/v)). Both mobile phases A and B contained 5-mM ammonium acetate. The samples were placed on a VX-2500 tube vortexer (VWR International, LLC, Radnor, PA) for 5 minutes and then centrifuged for 4 minutes at 6,500g (Beckman Coulter, Brea, CA). The resultant supernatant was transferred into high-performance liquid chromatography vials for analysis. GL-1 and galactosylceramide were separated using a Waters Acquity UPLC and Atlantis HILIC Silica column (2.1 mm \times 150 mm, 3- μ m particles, Waters Corp., Milford, MA) and analyzed by an API 5000 triple quadrupole mass spectrometer in MRM mode (Applied Biosystems, Foster City, CA).

For lyso-GL-1 analysis, 25 μ l of brain homogenates or 30 μ l of liver homogenates were extracted with 1 ml of 50% of mobile phase A and 50% of mobile phase B. After extraction, the supernatant was transferred into high-performance liquid chromatography vials. Lyso-GL-1 and psychosine were separated using an Agilent 1290 Infinity LC system and a Waters BEH HILIC column (2.1 mm \times 100 mm, 1.7- μ m particles), and analyzed by an Agilent 6490 triple quadrupole mass spectrometer in MRM mode (Agilent Technologies, Santa Clara, CA). The mobile phases used for lyso-GL-1 and psychosine separation consisted of 95:5 acetonitrile/200-mM ammonium acetate (v/v) and 95:5 methanol/200-mM ammonium acetate (v/v) at pH 9.0. GL-1 standards were purchased from Matreya, LLC (Pleasant Gap, PA) and lyso-GL-1 standards from Avanti Polar Lipids (Alabaster, AL).

Histology, immunohistochemistry (IHC), and quantitative histomorphometry. Animals subjected to CBE treatment were killed by CO₂ asphyxiation and transcardially perfused with saline, formalin fixed, and paraffin embedded. Sagittal sections of brain were stained with hematoxylin and eosin and then examined microscopically. Unstained serial sections were subjected to brightfield IHC to detect microglia/macrophages. Detection was performed using a rat antimouse CD68 antibody (Abcam, Cambridge, MA; catalog# ab53444) and a BondMax automated immunostainer (Leica Biosystems, Buffalo Grove, IL). A rat IgG_{2a} antibody (Serotec, Raleigh, NC; catalog #MCA1212) was used as an isotype control. To localize astrocytes, unstained serial sections were immunostained with a rabbit anti-GFAP antibody (Dako, Carpinteria, CA; catalog #Z0334). Rabbit IgG (Jackson ImmunoResearch, West Grove, PA; catalog # 011-000-003) was used as an isotype control. Immunostaining was visualized using the DAB-based Bond Polymer Refine detection kit (Leica).

Immunostained slides were scanned using a 20 \times objective lens in a Mirax scanner (Carl Zeiss, Thornwood, NY). Scanned images were subjected to quantitative histomorphometry using the HALO image analysis software (Indica Labs, Corrales, NM). The images were annotated to select regions of interest such as the cortex, striatum, hippocampus, substantia nigra, and cerebellum. Automated area quantitation algorithms were generated using HALO for specific detection of anti-CD68- or anti-GFAP-stained tissues within these regions of interests. Percent immunopositive areas within each regions of interest were obtained as quantitative IHC data.

For studies using the 4L;C* mice, animals were killed by CO₂ asphyxiation and transcardially perfused with saline. The tissues were dissected and fixed in 10% formalin or 4% paraformaldehyde, and processed for paraffin or frozen blocks, respectively. Hematoxylin and eosin and anti-CD68 antibody staining were carried out as previously described.¹⁰ The Discovery XT Staining Module on BenchMark XT Automated IHC/ISH slide staining system (Ventana Medical System, Tucson, AZ) was used for immunohistochemical analysis of sections stained with the anti-CD68 antibody. Frozen tissue sections fixed with 4% paraformaldehyde were incubated with a rat antimouse CD68 monoclonal antibody (1/3000 in DISCOVERY Antibody diluent) and detected with biotinylated rabbit antirat IgG (H+L) (1/100 in DISCOVERY Antibody diluent). Detection

was performed using the Ventana IHC DAB Map Kit. Tissue sections were counterstained with hematoxylin and analyzed by light microscopy. Representative 100× digital images were subjected to CD68-positive area quantification using HALO software as described above.

ACKNOWLEDGMENTS

The authors thank Nick Panarello, Leah Curtin, and members of the Comparative Medicine department, and Venette Inskeep, Ryan Apel, and Benjamin Liou in Division of Human Genetics at Cincinnati Children's Hospital Medical Center for their assistance with animal studies. We would also like to acknowledge the members of the Histology and Pathology departments for their expertise in processing the tissue samples, and members of the Chemistry department (Ray Gimi, Jin Zhao, Paul Konowicz, and Mike Reardon) for the synthesis and purification of Genz-682452. John Marshall, Dinesh Bangari, Eva Budman, Hyejung Park, Jennifer Nietupski, Amy Allaire, Mary Cromwell, Bing Wang, John Leonard, and Seng Cheng are all shareholders of Sanofi S.A. stock and/or employees of Sanofi. Ying Sun has research support from both Genzyme, Inc. and Lysosomal Therapeutics, Inc. The terms of these individual arrangements have been reviewed and approved by Cincinnati Children's Hospital Medical Center in accordance with its policy on objectivity in research. Gregory A. Grabowski, an independent contractor/consultant, is currently a consultant to Alexion Pharmaceuticals, Lysosomal Therapeutics, Inc. and a member of the Scientific Advisory Board of Lysosomal Therapeutics. He is also an Adjunct Professor of Pediatrics at the University of Cincinnati and of Human Genetics at the Cincinnati Children's Hospital Medical Center. He was formerly CSO for Synageva BioPharma Corp. In the past 5 years, he has been a consultant to Genzyme Corp. and a *pro bono* member of the Project Expert Committee to Genzyme Corp. and Shire in philanthropic activities related to enzyme therapy for Gaucher disease.

REFERENCES

- Grabowski, GA, Petsko, GA and Kolodny, EH (2010). Gaucher disease. In: Valle, D, Beaudet, A, Vogelstein, B, Kinzler, K, Antonarakis, S, Ballabio, A et al. (eds.). *The Online Metabolic and Molecular Bases of Inherited Disease*. McGraw-Hill Medical: New York. Part 16, ch. 146.
- Weinreb, NJ, Charrow, J, Andersson, HC, Kaplan, P, Kolodny, EH, Mistry, P et al. (2002). Effectiveness of enzyme replacement therapy in 1028 patients with type 1 Gaucher disease after 2 to 5 years of treatment: a report from the Gaucher Registry. *Am J Med* **113**: 112–119.
- Grabowski, GA, Kacena, C, Cole, JA, Hollak, CE, Zhang, L, Yee, J et al. (2009). Dose–response relationships for enzyme replacement therapy with imiglucerase/algucerase in patients with Gaucher disease type 1. *Genet Med* **11**: 92–100.
- Cox, TM, Aerts, JM, Andria, G, Beck, M, Belmatoug, N, Bembé, B et al.; Advisory Council to the European Working Group on Gaucher Disease (2003). The role of the iminosugar N-butyldeoxyinosimycin (miglustat) in the management of type I (non-neuronopathic) Gaucher disease: a position statement. *J Inher Metab Dis* **26**: 513–526.
- Smid, BE and Hollak, C (2014). A systematic review on effectiveness and safety of eliglustat for type 1 Gaucher disease. *Expert Opinion on Orphan Drugs* (doi: 10.1517/21678707.2014.899148).
- Weiss, K, Gonzalez, AN, Lopez, G, Pedeoim, L, Groden, C and Sidransky, E (2015). The clinical management of Type 2 Gaucher disease. *Mol Genet Metab* **114**: 110–122.
- Davies, EH, Erikson, A, Collin-Histed, T, Mengel, E, Tylki-Szymanska, A and Vellodi, A (2007). Outcome of type III Gaucher disease on enzyme replacement therapy: review of 55 cases. *J Inher Metab Dis* **30**: 935–942.
- Davies, EH, Mengel, E, Tylki-Szymanska, A, Kleinotiene, G, Reinke, J and Vellodi, A (2011). Four-year follow-up of chronic neuronopathic Gaucher disease in Europeans using a modified severity scoring tool. *J Inher Metab Dis* **34**: 1053–1059.
- Zimran, A and Elstein, D (2007). No justification for very high-dose enzyme therapy for patients with type III Gaucher disease. *J Inher Metab Dis* **30**: 843–844.
- Burrow, TA, Sun, Y, Prada, CE, Bailey, L, Zhang, W, Brewer, A et al. (2015). CNS, lung, and lymph node involvement in Gaucher disease type 3 after 11 years of therapy: clinical, histopathologic, and biochemical findings. *Mol Genet Metab* **114**: 233–241.
- Bembé, B, Ciana, G and Zanatta, M (2005). Cerebrospinal fluid infusion of algucerase in the treatment of acute neuronopathic Gaucher's disease. *Pediatr. Res* **38**: 425.
- Lonser, RR, Schiffman, R, Robison, RA, Butman, JA, Quezado, Z, Walker, ML et al. (2007). Image-guided, direct convective delivery of glucocerebrosidase for neuronopathic Gaucher disease. *Neurology* **68**: 254–261.
- Ringdén, O, Groth, CG, Erikson, A, Granqvist, S, Månsson, JE and Sparrelid, E (1995). Ten years' experience of bone marrow transplantation for Gaucher disease. *Transplantation* **59**: 864–870.
- Machaczka, M (2013). Allogeneic hematopoietic stem cell transplantation for treatment of Gaucher disease. *Pediatr Hematol Oncol* **30**: 459–461.
- Parenti, G, Pignata, C, Vajro, P and Salerno, M (2013). New strategies for the treatment of lysosomal storage diseases (review). *Int J Mol Med* **31**: 11–20.
- Schönemann, W, Gallienne, E, Ikeda-Obatake, K, Asano, N, Nakagawa, S, Kato, A et al. (2013). Glucosylceramide mimics: highly potent GCase inhibitors and selective pharmacological chaperones for mutations associated with types 1 and 2 Gaucher disease. *ChemMedChem* **8**: 1805–1817.
- Schiffmann, R, Fitzgibbon, EJ, Harris, C, DeVile, C, Davies, EH, Abel, L et al. (2008). Randomized, controlled trial of miglustat in Gaucher's disease type 3. *Ann Neurol* **64**: 514–522.
- Lukina, E, Watman, N, Arreguin, EA, Banikazemi, M, Dragosky, M, Iastrebner, M et al. (2010). A phase 2 study of eliglustat tartrate (Genz-112638), an oral substrate reduction therapy for Gaucher disease type 1. *Blood* (doi: 10.1182/blood-2010-03-273151).
- McEachern, KA, Fung, J, Komamitsky, S, Siegel, CS, Chuang, WL, Hutto, E et al. (2007). A specific and potent inhibitor of glucosylceramide synthase for substrate inhibition therapy of Gaucher disease. *Mol Genet Metab* **91**: 259–267.
- Marshall, J, McEachern, KA, Chuang, WL, Hutto, E, Siegel, CS, Shayman, JA et al. (2010). Improved management of lysosomal glucosylceramide levels in a mouse model of type 1 Gaucher disease using enzyme and substrate reduction therapy. *J Inher Metab Dis* **33**: 281–289.
- Cabrera-Salazar, MA, Deriso, M, Bercury, SD, Li, L, Lydon, JT, Weber, W et al. (2012). Systemic delivery of a glucosylceramide synthase inhibitor reduces CNS substrates and increases lifespan in a mouse model of type 2 Gaucher disease. *PLoS One* **7**: e43310.
- Ashe, KM, Budman, E, Bangari, DS, Siegel, CS, Nietupski, JB, Wang, B et al. (2015). Efficacy of enzyme and substrate reduction therapy with a novel antagonist of glucosylceramide synthase for fabry disease. *Mol Med* **21**: 389–399.
- Ito, S and Barrett, AJ (2013). Gauchers disease—a reappraisal of hematopoietic stem cell transplantation. *Pediatr Hematol Oncol* **30**: 61–70.
- Premkumar, L, Sawkar, AR, Boldin-Adamsky, S, Toker, L, Silman, I, Kelly, JW et al. (2005). X-ray structure of human acid-beta-glucosidase covalently bound to conduritol-B-epoxide. Implications for Gaucher disease. *J Biol Chem* **280**: 23815–23819.
- Kanfer, JN, Legler, G, Sullivan, J, Raghavan, SS and Mumford, RA (1975). The Gaucher mouse. *Biochem Biophys Res Commun* **67**: 85–90.
- Stephens, MC, Bernatsky, A, Burachinsky, V, Legler, G and Kanfer, JN (1978). The Gaucher mouse: differential action of conduritol B epoxide and reversibility of its effects. *J Neurochem* **30**: 1023–1027.
- Xu, YH, Reboulet, R, Quinn, B, Huelsken, J, Witte, D and Grabowski, GA (2008). Dependence of reversibility and progression of mouse neuronopathic Gaucher disease on acid beta-glucosidase residual activity levels. *Mol Genet Metab* **94**: 190–203.
- Mucci, JM, Suqueli García, F, de Francesco, PN, Ceci, R, Di Genaro, S, Fossati, CA et al. (2013). Uncoupling of osteoblast-osteoclast regulation in a chemical murine model of Gaucher disease. *Gene* **532**: 186–191.
- Ridley, CM, Thur, KE, Shanahan, J, Thillaiappan, NB, Shen, A, Uhl, K et al. (2013). β -Glucosidase 2 (GBA2) activity and imino sugar pharmacology. *J Biol Chem* **288**: 26052–26066.
- Sun, Y, Liou, B, Ran, H, Skelton, MR, Williams, MT, Vorhees, CV et al. (2010). Neuronopathic Gaucher disease in the mouse: viable combined selective saposin C deficiency and mutant glucocerebrosidase (V394L) mice with glucosylsphingosine and glucosylceramide accumulation and progressive neurological deficits. *Hum Mol Genet* **19**: 1088–1097.
- Kanfer, JN, Stephens, MC, Singh, H and Legler, G (1982). The Gaucher mouse. *Prog Clin Biol Res* **95**: 627–644.
- Yoneshige, A, Suzuki, K, Suzuki, K and Matsuda, J (2010). A mutation in the saposin C domain of the sphingolipid activator protein (Prosaposin) gene causes neurodegenerative disease in mice. *J Neurosci Res* **88**: 2118–2134.
- Yang, WW, Sidman, RL, Taksir, TV, Treleavan, CM, Fidler, JA, Cheng, SH et al. (2011). Relationship between neuropathology and disease progression in the SOD1(G93A) ALS mouse. *Exp Neurol* **227**: 287–295.
- Lin, CH, Tallaksen-Greene, S, Chien, WM, Cearley, JA, Jackson, WS, Crouse, AB et al. (2001). Neurological abnormalities in a knock-in mouse model of Huntington's disease. *Hum Mol Genet* **10**: 137–144.
- Vitner, EB, Vardi, A, Cox, TM and Futerman, AH (2015). Emerging therapeutic targets for Gaucher disease. *Expert Opin Ther Targets* **19**: 321–334.
- Sun, Y, Ran, H, Liou, B, Quinn, B, Zamzow, M, Zhang, W et al. (2011). Isogomine *in vivo* effects in a neuronopathic Gaucher disease mouse. *PLoS One* **6**: e19037.
- Benito, JM, García Fernández, JM and Ortiz Mellet, C (2011). Pharmacological chaperone therapy for Gaucher disease: a patent review. *Expert Opin Ther Pat* **21**: 885–903.
- Cabrera-Salazar, MA, Bercury, SD, Ziegler, RJ, Marshall, J, Hodges, BL, Chuang, WL et al. (2010). Intracerebroventricular delivery of glucocerebrosidase reduces substrates and increases lifespan in a mouse model of neuronopathic Gaucher disease. *Exp Neurol* **225**: 436–444.
- Farfel-Becker, T, Vitner, EB and Futerman, AH (2011). Animal models for Gaucher disease research. *Dis Model Mech* **4**: 746–752.
- Zigdon, H, Meshcheriakova, A and Futerman, AH (2014). From sheep to mice to cells: tools for the study of the sphingolipidoses. *Biochim Biophys Acta* **1841**: 1189–1199.
- Marshall, J, McEachern, KA, Kyros, JA, Nietupski, JB, Budzinski, T, Ziegler, RJ et al. (2002). Demonstration of feasibility of *in vivo* gene therapy for Gaucher disease using a chemically induced mouse model. *Mol Ther* **6**: 179–189.
- Vitner, EB, Salomon, R, Farfel-Becker, T, Meshcheriakova, A, Ali, M, Klein, AD et al. (2014). RPK3 as a potential therapeutic target for Gaucher's disease. *Nat Med* **20**: 204–208.
- Sun, Y, Zhang, W, Xu, YH, Quinn, B, Dasgupta, N, Liou, B et al. (2013). Substrate compositional variation with tissue/region and Gba1 mutations in mouse models—implications for Gaucher disease. *PLoS One* **8**: e57560.
- Hara, A and Radin, NS (1979). Destruction and resynthesis of mouse beta-glucosidases. *Biochim Biophys Acta* **582**: 412–422.
- Ben-David, O and Futerman, AH (2010). The role of the ceramide acyl chain length in neurodegeneration: involvement of ceramide synthases. *Neuromolecular Med* **12**: 341–350.
- Orvisky, E, Sidransky, E, McKinney, CE, Lamarca, ME, Samimi, R, Krasnewich, D et al. (2000). Glucosylsphingosine accumulation in mice and patients with type 2 Gaucher disease begins early in gestation. *Pediatr Res* **48**: 233–237.

47. Schueler, UH, Kolter, T, Kaneski, CR, Blusztajn, JK, Herkenham, M, Sandhoff, K *et al.* (2003). Toxicity of glucosylsphingosine (glucopsychosine) to cultured neuronal cells: a model system for assessing neuronal damage in Gaucher disease type 2 and 3. *Neurobiol Dis* **14**: 595–601.
48. Nilsson, O and Svennerholm, L (1982). Accumulation of glucosylceramide and glucosylsphingosine (psychosine) in cerebrum and cerebellum in infantile and juvenile Gaucher disease. *J Neurochem* **39**: 709–718.
49. Orvisky, E, Park, JK, LaMarca, ME, Ginns, EI, Martin, BM, Tayebi, N *et al.* (2002). Glucosylsphingosine accumulation in tissues from patients with Gaucher disease: correlation with phenotype and genotype. *Mol Genet Metab* **76**: 262–270.
50. Farfel-Becker, T, Vitner, EB, Kelly, SL, Bame, JR, Duan, J, Shinder, V *et al.* (2014). Neuronal accumulation of glucosylceramide in a mouse model of neuronopathic Gaucher disease leads to neurodegeneration. *Hum Mol Genet* **23**: 843–854.
51. Vitner, EB, Farfel-Becker, T, Eilam, R, Biton, I and Futerman, AH (2012). Contribution of brain inflammation to neuronal cell death in neuronopathic forms of Gaucher's disease. *Brain* **135**: 1724–1735.
52. Wraith, JE, Vecchio, D, Jacklin, E, Abel, L, Chadha-Boreham, H, Luzy, C *et al.* (2010). Miglustat in adult and juvenile patients with Niemann–Pick disease type C: long-term data from a clinical trial. *Mol Genet Metab* **99**: 351–357.
53. Benko, W, Ries, M, Wiggs, EA, Brady, RO, Schiffmann, R and Fitzgibbon, EJ (2011). The saccadic and neurological deficits in type 3 Gaucher disease. *PLoS One* **6**: e22410.
54. Gornati, R, Berra, B, Montorfano, G, Martini, C, Ciana, G, Ferrari, P *et al.* (2002). Glycolipid analysis of different tissues and cerebrospinal fluid in type II Gaucher disease. *J Inherit Metab Dis* **25**: 47–55.
55. Zigdon, H, Savidor, A, Levin, Y, Meshcheriakova, A, Schiffmann, R and Futerman, AH (2015). Identification of a biomarker in cerebrospinal fluid for neuronopathic forms of Gaucher disease. *PLoS One* **10**: e0120194.
56. Schultheis, PJ, Fleming, SM, Clippinger, AK, Lewis, J, Tsunemi, T, Giasson, B *et al.* (2013). Atp1 3a2-deficient mice exhibit neuronal ceroid lipofuscinosis, limited α -synuclein accumulation and age-dependent sensorimotor deficits. *Hum Mol Genet* **22**: 2067–2082.



This work is licensed under a Creative Commons Attribution-NonCommercial-NoDerivs 4.0 International License. The images or other third party material in this article are included in the article's Creative Commons license, unless indicated otherwise in the credit line; if the material is not included under the Creative Commons license, users will need to obtain permission from the license holder to reproduce the material. To view a copy of this license, visit <http://creativecommons.org/licenses/by-nc-nd/4.0/>